

PdCo bimetallic nanoparticles supported on PPI-grafted graphene as an efficient catalyst for Sonogashira reactions

Cite this: DOI: 10.1039/c3ta11706e

Ahmad Shaabani* and Mojtaba Mahyari

Received 30th April 2013
Accepted 29th May 2013

DOI: 10.1039/c3ta11706e

www.rsc.org/MaterialsA

A highly active catalyst based on PdCo alloy nanoparticles supported on polypropylenimine dendrimers, grown on graphene nanosheets, was synthesized and used for carbon–carbon cross-coupling Sonogashira reactions. The prepared catalyst facilitated a facile, efficient and environmentally friendly procedure for the Sonogashira reaction under copper and solvent free conditions using ultrasound irradiation at room temperature. The results showed that the catalyst could be easily recovered and reused several times without significant loss of activity.

Introduction

After the successful isolation of single sheets of graphene in 2004, graphene has received much attention in many fields because of its interesting electrical, optical and electrochemical properties.^{1–3} Graphene, due to its high specific surface area, extraordinary thermal and mechanical properties, and high stability to different conditions has been thought to be an ideal support in heterogeneous catalysis.^{4–10} However, stabilization of nanoparticles on graphene and achievement of uniform distributions are two barriers to overcome, largely affected by the metal–graphene interaction and the chemical inertness of graphene. There are different methods available to deal with these challenges. One of the most important methods involves functionalizing graphene with polymers, which also allows one to obtain chemically processable graphene.^{11–15} A well defined polymer known as a dendrimer^{16,17} can be used as a template to control the size, stability and solubility of nanoparticles ranging in diameter from <1–5 nm. Dendrimers are suitable hosts for metal nanoparticles, especially for catalytic systems, for the following reasons: (i) the nanoparticles are stabilized by encapsulation within the dendrimer and do not agglomerate;^{18–24} (ii) the encapsulated nanoparticles are confined by steric effects, therefore a substantial fraction of their surface is unpassivated and available to take part in catalytic reactions.^{19,20,22–24} Poly-amidoamine (PAMAM) and polypropylenimine (PPI) dendrimers are the most widely used dendrimers in various applications, however PPI dendrimers are stable at very high temperatures, whereas PAMAM dendrimers undergo retro-Michael addition at temperatures higher than 100 °C.²⁵

Bimetallic nanoparticles (NPs) are an important class of catalysts. Bimetallic nanoparticles can be divided into three

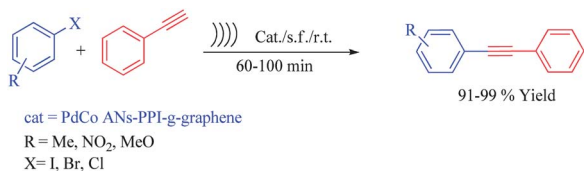
main types, according to their mixing pattern:²⁶ hetero-structures, core–shell structures, and intermetallic or alloyed structures. Among these types, bimetallic alloy NPs are very important nanomaterials because of their applications in a large variety of catalytic reactions, including catalytic alcohol oxidation, reforming reactions, and pollution control.^{27–34} The addition of a second metal is an important approach for tailoring the geometric and electronic structures of NPs, promoting their catalytic activity and selectivity.

One of the most important applications of nanoparticles stabilized on graphene is in heterogeneous catalysis for cross-coupling reactions, a cornerstone set of reactions in the formation of carbon–carbon bonds.^{35–38} One well known cross-coupling reaction is the Sonogashira protocol which is used to couple terminal alkynes with aryl halides for the production of aryl acetylenes and conjugated enynes.^{39–43} To date there have only been a few reports of PdCo alloy nanoparticles as catalysts for the Sonogashira cross-coupling reaction. Recently, Li *et al.*^{44,45} reported a new strategy involving hollow PdCo alloy nanospheres as a catalyst for Sonogashira reactions in water as a solvent at 80 °C with reaction times of 4–9 h.

Our approach was guided by three imperatives: (i) the support should control nanoparticle size and facilitate uniform distribution of the nanoparticles; (ii) the catalyst should be thermally stable and also air stable at room temperature, allowing its storage in normal bottles with unlimited shelf-life; and (iii) the catalyst should provide an efficient, environmentally benign and facile synthetic process for the Sonogashira coupling reaction.

In a continuation of our efforts to introduce new and efficient catalysts for various organic transformations,^{46–51} in this work, PPI dendrimer was grown to the third generation, on the surface of functionalized graphene using a divergent strategy, PdCo alloy nanoparticles were then attached *via* a co-complexation method. The efficiency of the prepared catalyst, polypropylenimine

Shahid Beheshti University, Department of Chemistry, P. O. Box 19396-4716, Tehran, Islamic Republic of Iran. E-mail: a-shaabani@sbu.ac.ir



Scheme 1 Sonogashira cross-coupling with PdCo ANP-PPI-g-graphene hybrid material.

grafted graphene (PdCo ANP-PPI-g-graphene), was investigated in Sonogashira cross-coupling reactions. The reaction was carried out in the presence of a catalytic amount of the synthesized alloy catalyst at room temperature under ultrasound irradiation and solvent free conditions (Scheme 1).

Experimental

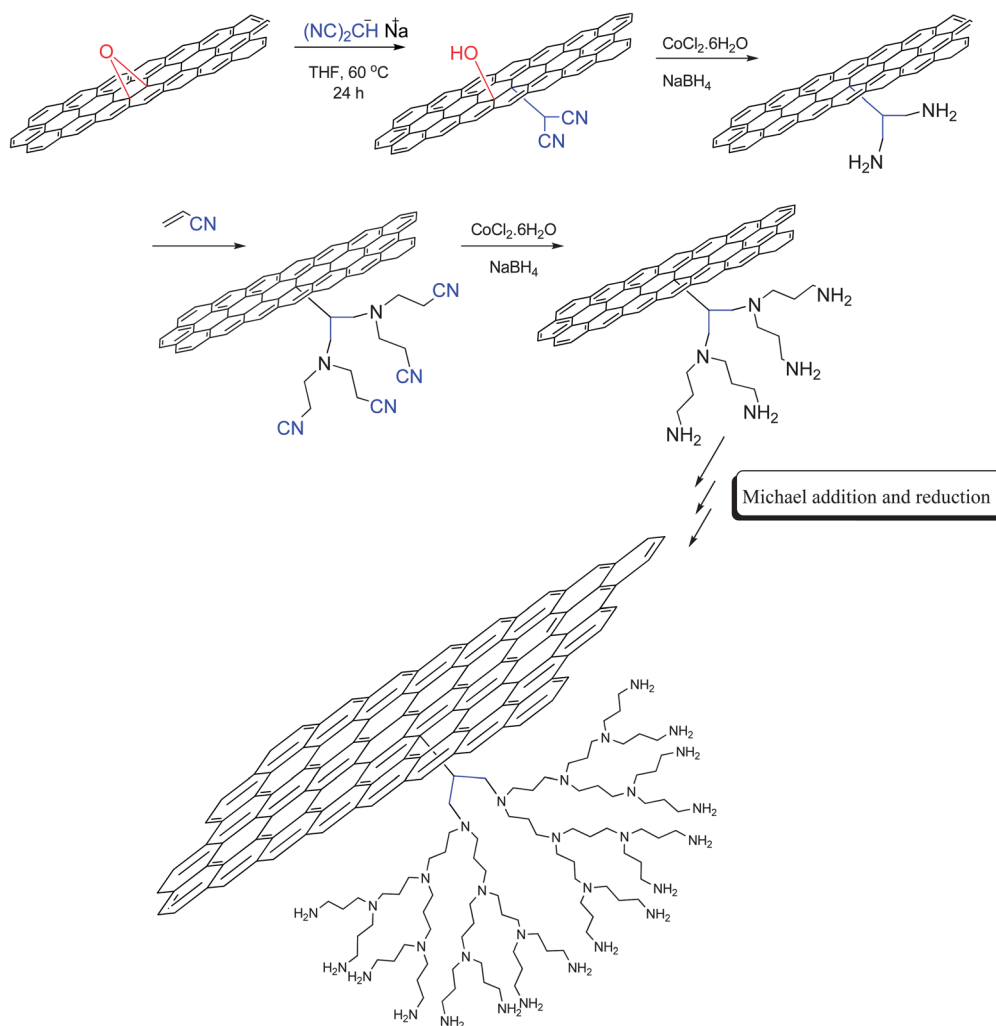
Instruments

An AA-680 Shimadzu (Kyoto, Japan) flame atomic absorption spectrometer (AAS) with a deuterium background corrector was used for determination of Pd(0) and Co(0). ¹H NMR spectra were recorded with a BRUKER DRX-300 AVANCE spectrometer, and

DMSO-d₆ was used as a solvent. IR spectra were recorded on a Bomem MB-Series FT-IR spectrophotometer. High resolution transmission electron microscopy (HR-TEM) analysis was performed using a ZEISS EM-900 at an acceleration voltage of 80 kV. Catalysis products were analyzed using a Varian 3900 GC (GC conversion was obtained from the ratio of aryl halide to authentic product, using *n*-decane as an internal standard). An ultrasonic bath (EUROSONIC® 4D ultrasound cleaner with a frequency of 25 kHz) was used to disperse materials in solvent. PPI dendrimer is commercially available from Aldrich Chemical Company. Thermogravimetric analysis (TGA) was carried out using an STA 1500 instrument at a heating rate of 10 °C min⁻¹ in air. X-ray powder diffraction (XRD) data were collected on an XD-3A diffractometer using Cu K α radiation. XPS analysis was performed using a VG multilab 2000 spectrometer (ThermoVG scientific) in an ultra high vacuum.

Synthesis of PdCo ANP-PPI-g-graphene hybrid material

Preparation of 1,3-diamine functionalized graphene oxide. Graphene oxide (GO)⁵² and malononitrile functionalized graphene, were synthesized by previously reported methods.⁵³



Scheme 2 Synthesis route for PPI dendrimer growth on graphene.

Table 1 Amount of -NH_2 group and Pd(0) and Co(0) on each generation of the PdCo ANP-PPI-*g*-graphene hybrid material

Entry	Generation	-NH_2^a content (mmol g^{-1})	Amount of Pd(0) ^b (mmol g^{-1})	Amount of Co(0) ^b (mmol g^{-1})
1	0	0.27	0.14	0.10
2	1	0.40	0.20	0.13
3	2	0.75	0.36	0.29
4	3	1.02	0.48	0.40

^a Determined by titration. ^b Determined by AAS.

Firstly, malononitrile functionalized graphene (1.0 g) was reduced using $\text{CoCl}_2 \cdot 6\text{H}_2\text{O}$ (23.8 g, 0.1 mol) and NaBH_4 (19.0 g, 0.5 mol) in MeOH (300.0 mL) at 20 °C for 24 h. Then, the reaction mixture was acidified with HCl (3 N, 100.0 mL) and stirred at ambient temperature for 4 days to ensure reaction completion. The product was filtered under vacuum, washed with ethanol and water, and dried under vacuum at 50 °C for 24 h.

Preparation of PPI-*g*-graphene hybrid material. First, second and third generation PPI dendrimers were synthesized on the amino functionalized graphene. The amino functionalized graphene (0.8 g) was added in portions, at ambient temperature with stirring, to acrylonitrile (3.4 mL, 80.0 mmol) and methanol (10.0 mL) in a 100 mL round bottomed flask. The reaction mixture was stirred at ambient temperature under a nitrogen atmosphere for 5 days. After completion of the reaction, excess reactant and solvent were removed under vacuum. The product was washed with methanol and acetone. It was dried under vacuum for 24 h. Then, $\text{CoCl}_2 \cdot 6\text{H}_2\text{O}$ (23.8 g, 0.1 mol) in MeOH (300.0 mL) and NaBH_4 (19.0 g, 0.5 mol) were added to the reaction mixture and stirred at 20 °C for 24 h. After that, the mixture was acidified with HCl (3 N, 100.0 mL) and stirred at ambient temperature for 4 days (Scheme 2). Next, the product was filtered under vacuum, washed with ethanol and water and dried under vacuum at 50 °C for 4 h.^{54,55} Then, the amount of

free primary amine in the periphery of the dendrimer was measured by titration (Table 1).⁵⁶

Preparation of PdCo ANP-PPI-*g*-graphene hybrid material.

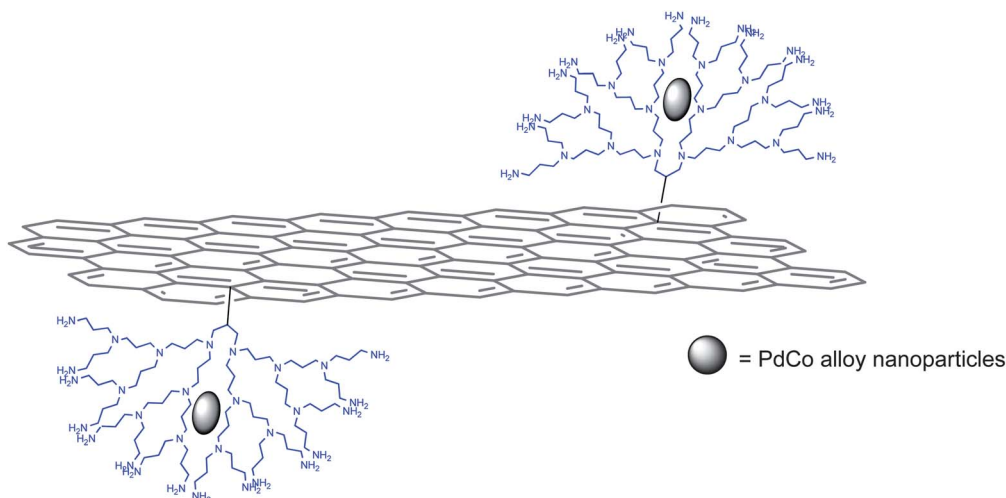
First, an aqueous solution of PdCl_2 (0.1 g in 3.0 mL) and PPI-*g*-graphene (0.2 g in 10.0 mL) were mixed and placed in an ultrasonic bath (25 kHz) for 20 min to widely disperse the metal ions in the dendritic shells of the hybrid material. Then, an aqueous solution of $\text{CoCl}_2 \cdot 6\text{H}_2\text{O}$ (0.36 g in 3.0 mL) was added and placed in the ultrasonic bath for 20 min. Finally, a solution of NaBH_4 (1.0 M, 10.5 mL) in 0.3 M aqueous NaOH was added to the reaction mixture and stirred for 24 h. After completion of the reaction, the mixture was filtered under vacuum, washed well with water and ethanol and dried under vacuum at 50 °C for 4 h.

General procedure for the catalytic Sonogashira cross-coupling. A dry 10 mL flask was charged with an alkyne (1.0 mmol), an aryl halide (1.0 mmol), and PdCo ANP-PPI-*g*-graphene (0.004 g, 0.19 mol% Pd, 0.16 mol% Co) as catalyst and sonicated using an ultrasonic bath (frequency = 25 kHz) at 25 °C for a specified period of time (see Table 7). After completion of the reaction, as indicated by TLC (EtOAc : *n*-hexane, 1 : 3) diethyl ether was added to the reaction mixture and the catalyst was separated by centrifugation. Next, the reaction mixture was analyzed by gas chromatography using a CP-Sil-8 fused silica capillary column.

Results and discussion

PPI dendrimer growth on graphene and subsequent loading of palladium and cobalt have been outlined in Schemes 2 and 3. The PPI dendrimers (third generation) were grown on the surface of graphene to obtain the PPI-grafted graphene hybrid material by employing a divergent route starting from nitrile functionalized graphene.

The three generations of the dendrimer were characterised by FT-IR spectroscopy (Fig. 1). The broad band at 3430 cm^{-1} is due to the -NH_2 stretching, the absorptions at $2800\text{--}3000 \text{ cm}^{-1}$

**Scheme 3** Synthesis route of PdCo ANP-PPI-*g*-graphene hybrid material.

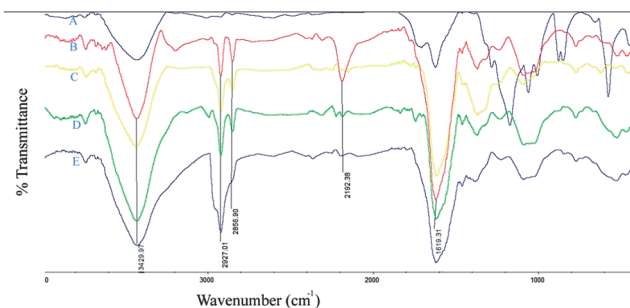


Fig. 1 FT-IR spectra for PPI dendrimer supported on graphene. GO (A), malonitrile functionalized graphene (B), first (C), second (D), and third (E) generations of PPI dendrimer on graphene.

are attributed to the C–H stretching of the CH_2 group and the band at 2192 cm^{-1} is assigned to the CN group, confirming malonitrile functionalized graphene (Fig. 1B). Increasing relative intensities of the above mentioned absorptions indicates that each generation of dendrimer was successfully constructed on the surface of graphene.

Thermogravimetric analysis (TGA) was then used to characterise the growth of dendrimer on the surface of the graphene (Fig. 2). The first decomposition starts between $100\text{--}200\text{ }^\circ\text{C}$ with a corresponding weight loss of water. The weight losses observed at $450\text{--}600\text{ }^\circ\text{C}$ on the TGA plots show average weight losses of 12%, 24%, and 35% for first (C), second (D) and third (E) generations of PPI dendrimer on graphene, respectively.

^1H NMR results provide valuable information on the functional groups in the third generation PPI-*g*-graphene samples in DMSO-d_6 . The hydrogen signals of the grafted dendritic units are clearly observable in the corresponding ^1H NMR spectrum. The most shielded signal at 1.1 ppm is attributed to $\text{CH}_2\text{CH}_2\text{CH}_2$ and the next signal at 2.9 ppm could be assigned to CH_2N . The peak at 5.2 ppm was assigned to NH_2 groups (Fig. 3).

TEM images of graphene oxide (Fig. 4A) and third generation PPI-grafted graphene containing PdCo alloy nanoparticles, show the uniform dispersion and the size distribution of the supported palladium and cobalt alloy nanoparticles on the dendrimer grafted graphene (Fig. 4B–D). Moreover, TEM analysis, indicated that the range of nanoparticles sizes is 2–3 nm.

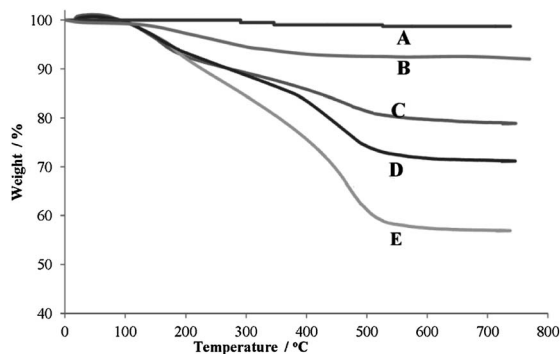


Fig. 2 Weight loss measured by TGA for PPI dendrimer supported on graphene. Pure graphite (A), graphene oxide (B) and first (C), second (D) and third (E) generations of PPI dendrimer on graphene.

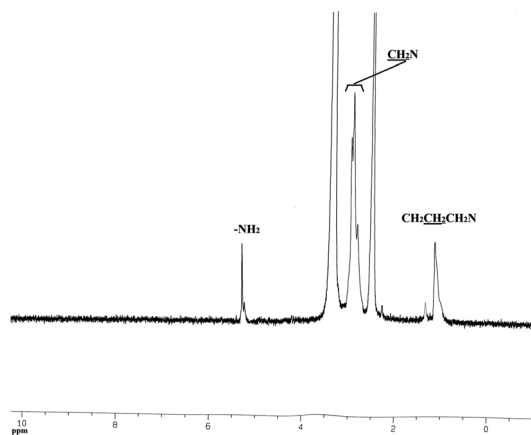


Fig. 3 ^1H NMR spectrum of graphene-supported dendrimer (third generation) in DMSO-d_6 .

The XPS spectrum of PdCo ANP-PPI-*g*-graphene is shown in Fig. 5. Since the sensitivity factor of Pd-3d is 2–3 times higher than that of Co-2p,⁵⁷ the peak area of Pd is larger than that of Co. The surface Pd and Co are found to be metallic, not oxides, by comparing experimental binding energies (Pd-3d_{5/2}: 334.6 eV, Co-2p_{3/2}: 777.5 eV) to those in the literature (Pd-3d_{5/2}: 334.4 eV, Co-2p_{3/2}: 781.5 eV). As for the binding energy of Co, the shift of the 2p_{3/2} peak to lower energy indicates alloying of Co with Pd.⁵⁸

As shown in Fig. 6 the XRD pattern of the third generation PdCo ANP-PPI-*g*-graphene hybrid material confirmed the crystalline structure of the PdCo alloy nanoparticles. The diffraction peaks for PdCo ANP-PPI-*g*-graphene were fairly broad,

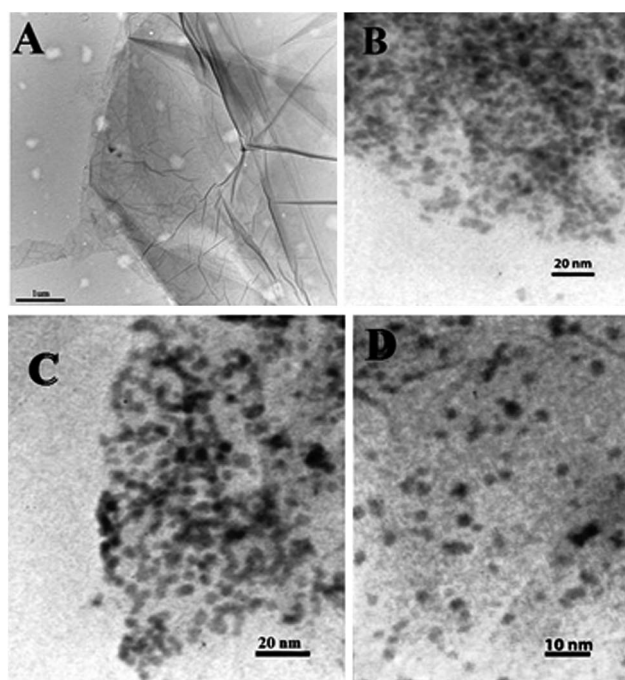


Fig. 4 HR-TEM images of graphene oxide (A), and PdCo nanoparticles on PPI-*g*-graphene (B–D).

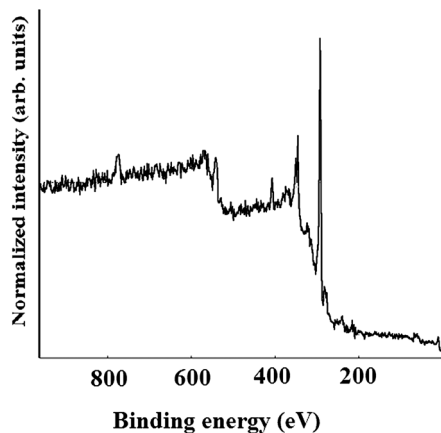


Fig. 5 XPS spectrum of PdCo ANP-PPI-g-graphene hybrid material.

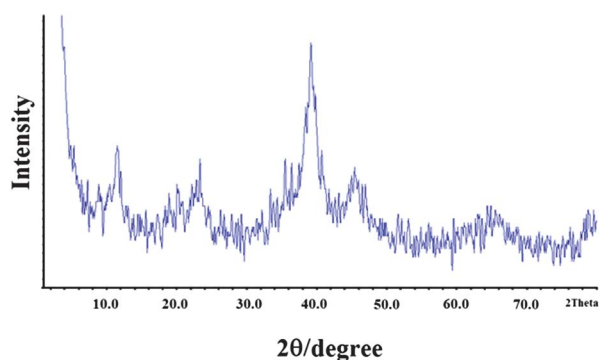


Fig. 6 X-ray diffraction (XRD) pattern of the PdCo ANP-PPI-g-graphene hybrid material.

indicating a nanocrystalline structure. The strong and sharp peak at $2\theta = 11.7^\circ$ corresponds to an interlayer distance of 7.6 Å (0 0 2) of GO. Reduced graphene oxide shows a broad peak that can be fitted by using a Lorentzian function to three peaks centered at $2\theta = 20.17^\circ$, 23.78° and 25.88° , corresponding to interlayer distances of 4.47, 3.82 and 3.53 Å, respectively. The three peaks at 2θ values of approximately 40.02, 46.59, and 68.03 are characteristic of face centered cubic (fcc) crystalline Pd, corresponding to the planes (1 1 1), (2 0 0) and (2 2 0). Although cobalt can take two different crystal systems; hexagonal and fcc, the spectrum is similar to those of fcc Pd and the peaks originating from Co cannot be found.^{59,60}

Finally, a cobalt palladium alloy dendrimer supported catalyst has been prepared by the co-complexation method.⁶¹ As indicated in Table 1, with higher generations of PPI, the loading of Pd and Co nanoparticles increased. This can be attributed to an exponential increase in the number of amino groups with higher generations of dendrimer.

To evaluate the catalytic properties of this catalyst, cross-coupling of iodobenzene with phenylacetylene was performed as a model reaction. In preliminary studies, the reaction was carried out in the presence of various amounts of catalyst (Table 2). As the catalyst amount was increased (0.004 g, 0.19 mol% Pd, 0.16 mol% Co), the reaction went to completion at

Table 2 Influence of the amount of catalyst on the Sonogashira reaction^a

Entry	Amount of catalyst (g)	Pd(0) content (mol%)	Co(0) content (mol%)	Yield ^b (%)
1	0.002	0.09	0.08	36
2	0.003	0.14	0.12	61
3	0.004	0.19	0.16	99
4	0.005	0.23	0.20	99

^a Reaction conditions: phenylacetylene (1.0 mmol), iodobenzene (1.0 mmol) and base under solvent free conditions were sonicated at 25 °C for 1 h. ^b Yield determined by GC analysis.

Table 3 Effect of the solvent and base on Sonogashira cross-coupling reaction using PdCo ANP-PPI-g-graphene hybrid material as a catalyst^a

Entry	Solvent	Base	Yield ^b (%)
1	NMP	K ₂ CO ₃	94
2	DMF	K ₂ CO ₃	92
3	H ₂ O	K ₂ CO ₃	82
4	CH ₃ CN	K ₂ CO ₃	84
5	—	K ₂ CO ₃	99
6	—	Et ₃ N	82
7	—	NaOAc	85
8	—	Pyridine	78
9	—	—	70

^a Reaction conditions: iodobenzene (1.00 mmol), phenylacetylene (1.00 mmol), catalyst (0.004 g, 0.19 mol% Pd, 0.16 mol% Co) and base (0.5 mmol) were sonicated at 25 °C for 1 h. ^b Yield determined by GC analysis.

room temperature. In order to determine the best solvent, various solvents, including NMP, DMF, H₂O and CH₃CN as well as solvent free conditions were tested. As indicated in Table 3, solvent free conditions are the best suited to this reaction in terms of yield, ease of work up and compliance with green chemistry principles (Table 3, entries 1–5).

The influence of base on the reaction was also studied. As shown in Table 3, K₂CO₃ is the best suited base (Table 3, entries 5–9). It is important to note that we found a relatively good yield was obtained in the absence of base (Table 3, entry 9). This may be explained because the catalyst provides a basic environment for the reaction.

Table 4 The effect of temperature on the reaction time and yield (A) in the presence of ultrasonic irradiation and (B) under conventional solvent free conditions^a

Entry	Temp. (°C)	Time (min) for A	Yield ^b (%)	
			A	B ^c
1	25	60	99	20
2	50	45	—	48
3	65	35	—	60
4	80	25	—	95

^a Reaction conditions: iodobenzene (1.0 mmol), phenylacetylene (1.0 mmol), catalyst (0.004 g, 0.19 mol% Pd, 0.16 mol% Co) and K₂CO₃ (0.50 mmol). ^b Yield determined by GC analysis. ^c At 1 h.

The best results were obtained in the presence of 0.004 g (0.19 mol% Pd, 0.16 mol% Co) of catalyst and 50 mol% of K_2CO_3 under solvent free conditions with sonication at room temperature for 1 h (Table 3, entry 5). As indicated in Table 4, use of ultrasonic irradiation (A) compared to conventional heating (B) decreases the reaction time and temperature required to obtain high yields by a factor of approximately 3. According to the observations obtained, it can be seen that temperature and ultrasonic irradiation play important roles in increasing yield and decreasing reaction time. As a consequence, it is possible to select the most appropriate conditions for practical applications. If temperature is not important, the reaction can be completed at high temperature, however, if temperature is an important factor, energy can be supplied in the form of ultrasonic irradiation.

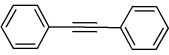
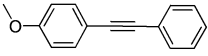
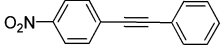
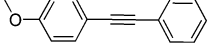
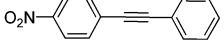
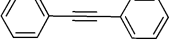
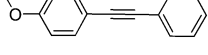
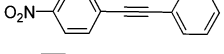
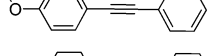
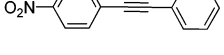
To confirm the activity and efficiency of PdCo ANP-PPI-g-graphene catalyst relative to corresponding individual nanoparticle (Pd or Co) catalysts, several examples of Sonogashira reactions have been examined. As indicated in Table 5 (entries 1–3), the catalytic Sonogashira reaction was significantly enhanced in the presence of the alloy PdCo as compared to each of the monometallic nanoparticles. However, because of the high cost of Pd, the industrial application of Sonogashira cross-coupling reaction is still limited. Obviously, to overcome this restriction, and to economize on expensive Pd metal in the preparation of active Pd catalyst, the design and synthesis of Pd/

non-noble-metal catalysts represent a promising approach. In addition, owing to the strong synergy between the metals, bimetallic alloy NPs have higher catalytic efficiencies than their monometallic counterparts. So, recent developments in synergistic catalysis for bimetallic alloy NPs will provide access to a variety of high performance and low cost catalysts for laboratory and industrial applications within the next few years.⁶²

To show the role and performance of graphene in PdCo ANP-PPI-g-graphene, PdCo ANP-PPI was also investigated in the Sonogashira reaction. As indicated in Table 5 (entries 3 and 4), the results are comparable in reaction yields and times. The metal loading of PPI-g-graphene and PPI are different. Actually, weight percent of metal (Pd and Co) in the PdCo ANP-PPI-g-graphene is approximately 21% w/w, while that of PdCo ANP-PPI is just 5%. So, to have a correct comparison we used a different amount of supported catalyst to give the same amount of metal nanoparticles, for example, the amount of supported catalyst for PdCo ANP-PPI-g-graphene was 0.004 g, but for PdCo ANP-PPI 0.017 g was used. Therefore, the metal loading on PPI-g-graphene is substantially more than PPI and consequently it has a cost limitation. Moreover, increasing the stability of the catalyst and facilitating the recovery process are the other advantages of using graphene as the support in this catalyst.

In order to investigate the scope and limitations of this catalyst in the Sonogashira cross-coupling reaction, a variety of

Table 5 Comparison of the results obtained from PdCo ANP-PPI-g-graphene with corresponding monometallic catalysts for Sonogashira coupling reactions^a

Entry	Cat.	Product	Time (h)	Yield ^b (%)
1	Pd NP-PPI-g-graphene		17	90
			17	85
			17	91
2	Co NP-PPI-g-graphene		30	10
			30	8
			30	12
3	PdCo ANP-PPI-g-graphene		1	99
			1.5	95
			1.5	99
4	PdCo ANP-PPI		1.5	95
			1.5	91
			1.5	96

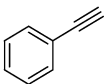
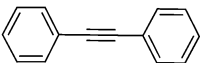
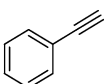
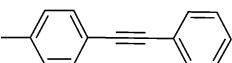
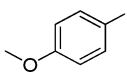
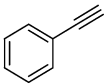
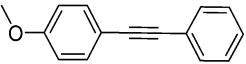
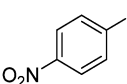
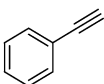
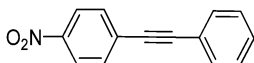
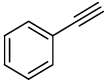
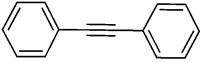
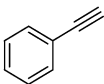
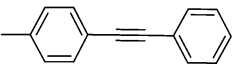
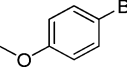
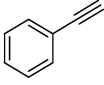
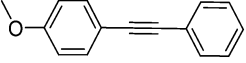
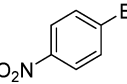
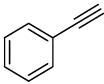
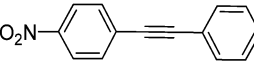
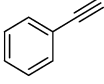
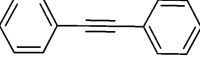
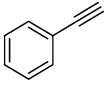
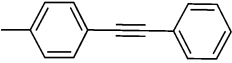
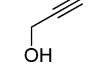
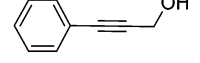
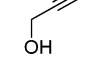
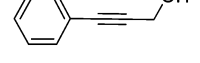
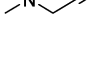
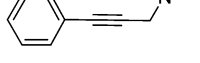
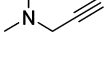
^a Reaction conditions: iodobenzene derivative (1.00 mmol), phenylacetylene (1.00 mmol), and K_2CO_3 (0.50 mmol) were sonicated at 25 °C. ^b Yield determined by GC analysis.

aryl bromides and iodides containing electron donating and electron withdrawing substituents with various terminal alkynes were screened under copper and solvent free conditions at room temperature. All products were obtained in high yields (Table 6). In view of the success of the above mentioned reactions, we decided to extend the study to aryl chlorides. As shown in Table 6 (entries 9 and 10), the reaction led to the formation of products in relatively good yields.

The results for our catalyst with respect to yields, solvents, temperature and reaction times, have been compared with previously reported palladium based catalysts. As shown in Table 7, in the case of PdCo ANP-PPI-g-graphene the reaction yield is higher in solvent free conditions at the shorter reaction time at room temperature.

The reusability of the catalyst was examined. After carrying out the reaction, the reaction mixture was filtered off and the

Table 6 PdCo ANP-PPI-g-graphene hybrid material catalyzed coupling of terminal alkynes with aryl halides^a

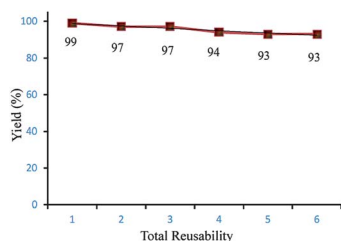
Entry	Aryl halide	Alkyne	Product	Time (h)	Yield ^b (%)
1				1	99
2				1	97
3				1.5	95
4				1.5	99
5				1.17	96
6				1.17	93
7				1.67	91
8				1	98
9				72	80
10				72	76
11				1.33	96
12				1.67	94
13				1	97
14				1.17	93

^a Reaction conditions: iodobenzene (1.00 mmol), phenylacetylene (1.00 mmol), catalyst (0.004 g, 0.19 mol% Pd, 0.16 mol% Co), and K₂CO₃ (0.50 mmol) were sonicated at 25 °C for 1 h. ^b Yield determined by GC analysis.

Table 7 Comparison of the results obtained from PdCo ANP–PPI-g-graphene with various types of palladium based catalysts for the Sonogashira coupling reaction

Entry	Cat.	Solvent	Temp. (°C)	Time (h)	Yield (%)	Ref.
1	PdCo ANP–PPI-g-graphene	None	25	1	99	—
2	Pd tripod nanocrystals	H ₂ O	100	6	93	63
3	Pd(0)/PVP	EtOH	80	6	95	64
4	Pd(0)/C ^a	DMA ^b	100	0.5	53	65
5	Pd(0)/C	i-PrOH/H ₂ O	80	6	67	66
6	PNP–SSS ^c	H ₂ O	100	3	95	67
7	Pd/GO ^d	i-PrOH/H ₂ O	80	24	95	68
8	CELL ^e -Pd(0)	CH ₃ CN	80	12	96	69

^a Carbon. ^b Dimethylacetamide. ^c Palladium nanoparticles on a silica–starch substrate. ^d Graphene oxide. ^e Cellulose.

**Fig. 7** The reusability of the catalyst.

catalyst separated as a black solid which was washed with diethyl ether (2 × 5 mL) and reused. Only minor decreases in the reaction yield were observed after six cycles (Fig. 7).

In conclusion, third generation PPI dendrimers were grown on the surface of functionalized graphene *via* a divergent method. The PPI-grafted graphene hybrid material was effectively employed as substrate for *in situ* generation of palladium cobalt alloy nanoparticles as a new heterogeneous catalyst for Sonogashira cross-coupling reactions. The reaction was carried out under environmentally benign, aerobic, and copper and solvent free conditions at room temperature. The new hybrid material, under optimal reaction conditions, was used as an efficient heterogeneous catalyst for couplings between a wide range of terminal alkynes and aryl halides in high yield. The structure of the catalyst was confirmed by TGA, XPS, XRD, IR. PdCo ANP–PPI-g-graphene hybrid material has advantages such as a uniform distribution of nanoparticles on the single layer graphene surface as indicated by TEM and good chemical stability in the reaction media proved by the reusability of the catalyst.

Acknowledgements

We gratefully acknowledge financial support from the Research Council of Shahid Beheshti University and Catalyst Center of Excellence (CCE).

References

- 1 K. Novoselov, A. Geim, S. Morozov, D. Jiang, Y. Zhang, S. Dubonos, I. Grigorieva and A. Firsov, *Science*, 2004, **306**, 666.
- 2 K. Novoselov, A. K. Geim, S. Morozov, D. Jiang, M. I. K. Grigorieva, S. Dubonos and A. Firsov, *Nature*, 2005, **438**, 197.
- 3 M. J. Allen, V. C. Tung and R. B. Kaner, *Chem. Rev.*, 2010, **110**, 132.
- 4 F. Schedin, A. Geim, S. Morozov, E. Hill, P. Blake, M. Katsnelson and K. Novoselov, *Nat. Mater.*, 2007, **6**, 652.
- 5 Y. Si and E. T. Samulski, *Nano Lett.*, 2008, **8**, 1679.
- 6 K. S. Novoselov, Z. Jiang, Y. Zhang, S. Morozov, H. Stormer, U. Zeitler, J. Maan, G. Boebinger, P. Kim and A. Geim, *Science*, 2007, **315**, 1379.
- 7 J. Wu, W. Pisula and K. Müllen, *Chem. Rev.*, 2007, **107**, 718.
- 8 E. Stolyarova, K. T. Rim, S. Ryu, J. Maultzsch, P. Kim, L. E. Brus, T. F. Heinz, M. S. Hybertsen and G. W. Flynn, *Proc. Natl. Acad. Sci. U. S. A.*, 2007, **104**, 9209.
- 9 Y. Zhang, Y. W. Tan, H. L. Stormer and P. Kim, *Nature*, 2005, **438**, 201.
- 10 M. Pumera, *Energy Environ. Sci.*, 2010, **4**, 668.
- 11 P. V. Kamat, *J. Phys. Chem. Lett.*, 2009, **1**, 520.
- 12 R. Muszynski, B. Seger and P. V. Kamat, *J. Phys. Chem. C*, 2008, **112**, 5263.
- 13 K. Jajuja, J. Linn, S. Melton and V. Berry, *J. Phys. Chem. Lett.*, 2010, **1**, 1853.
- 14 P. A. Pandey, G. R. Bell, J. P. Rourke, A. M. Sanchez, M. D. Elkin, B. J. Hickey and N. R. Wilson, *Small*, 2011, **7**, 3202.
- 15 P. Kundu, C. Nethravathi, P. A. Deshpande, M. Rajamathi, G. Madras and N. Ravishankar, *Chem. Mater.*, 2011, **23**, 2772.
- 16 E. Buhleier, W. Wehner and F. Vogtle, *Synthesis*, 1978, **155**, 158.
- 17 A. W. Bosman, H. M. Janssen and E. W. Meijer, *Chem. Rev.*, 1999, **99**, 1665.
- 18 M. Zhao, L. Sun and R. M. Crooks, *J. Am. Chem. Soc.*, 1998, **120**, 4877.
- 19 M. Zhao and R. M. Crooks, *Angew. Chem., Int. Ed.*, 1999, **38**, 364.
- 20 M. Zhao and R. M. Crooks, *Adv. Mater.*, 1999, **11**, 217.
- 21 M. Zhao and R. M. Crooks, *Chem. Mater.*, 1999, **11**, 3379.
- 22 L. K. Yeung and R. M. Crooks, *Nano Lett.*, 2001, **1**, 14.
- 23 V. Chechik, M. Zhao and R. M. Crooks, *J. Am. Chem. Soc.*, 1999, **121**, 4910.
- 24 V. Chechik and R. M. Crooks, *J. Am. Chem. Soc.*, 2000, **122**, 1243.
- 25 M. Zhao, Y. Liu, R. M. Crooks and D. E. Bergbreiter, *J. Am. Chem. Soc.*, 1999, **121**, 923.
- 26 D. S. Wang and Y. Li, *Adv. Mater.*, 2011, **23**, 1044.
- 27 H.-L. Jiang and Q. Xu, *J. Mater. Chem.*, 2011, **21**, 13705.

- 28 D. A. Hansgen, D. G. Vlachos and J. G. G. Chen, *Nat. Chem.*, 2010, **2**, 484.
- 29 X. Ji, K. T. Lee, R. Holden, L. Zhang, J. Zhang, G. A. Botton, M. Couillard and L. F. Nazar, *Nat. Chem.*, 2010, **2**, 286.
- 30 H. Kobayashi, M. Yamauchi, H. Kitagawa, Y. Kubota, K. Kato and M. Takata, *J. Am. Chem. Soc.*, 2010, **132**, 5576.
- 31 R. Ferrando, J. Jellinek and R. L. Johnston, *Chem. Rev.*, 2008, **108**, 845.
- 32 F. Studt, F. Abild-Pedersen, T. Bligaard, R. Z. Sørensen, C. H. Christensen and J. K. Nørskov, *Science*, 2008, **320**, 1320.
- 33 Y.-H. Tee, E. Grulke and D. Bhattacharyya, *Ind. Eng. Chem. Res.*, 2005, **44**, 7062.
- 34 B. Schrick, J. L. Blough, A. D. Jones and T. E. Mallouk, *Chem. Mater.*, 2002, **14**, 5140.
- 35 G. M. Scheuermann, L. Rumi, P. Steurer, W. Bannwarth and R. Mühlaupt, *J. Am. Chem. Soc.*, 2009, **131**, 8262.
- 36 Y. Li, X. Fan, J. Qi, J. Ji, S. Wang, G. Zhang and F. Zhang, *Mater. Res. Bull.*, 2010, **45**, 1413.
- 37 Y. Li, X. Fan, J. Qi, J. Ji, S. Wang, G. Zhang and F. Zhang, *Nano Res.*, 2010, **3**, 429.
- 38 J. Hu, Y. Wang, M. Han, Y. Zhou, X. Jiang and P. Sun, *Catal. Sci. Technol.*, 2012, **2**, 2332.
- 39 R. Chinchilla and C. Najera, *Chem. Soc. Rev.*, 2011, **40**, 5084.
- 40 S. Bhattacharya and S. Sengupta, *Meth. Org. Synth.*, 2004, **45**, 8733.
- 41 D. Mery, K. Heuze and D. Astruc, *Chem. Commun.*, 2003, 1934.
- 42 S. Santra, K. Dhara, P. Ranjan, P. Bera, J. Dash and S. K. Mandal, *Green Chem.*, 2011, **13**, 3238.
- 43 Y. F. Wang, W. Deng, L. Liu and Q. X. Guo, *Meth. Org. Synth.*, 2005, **25**, 8.
- 44 Y. Li, P. Zhou, Z. Dai, Z. Hu, P. Sun and J. Bao, *New J. Chem.*, 2006, **30**, 832.
- 45 H. Li, Z. Zhu, J. Liu, S. Xie and H. Li, *J. Mater. Chem.*, 2010, **20**, 4366.
- 46 S. Keshipour, S. Shojaei and A. Shaabani, *Cellulose*, 2013, **20**, 973.
- 47 A. Shaabani and E. Farhangi, *Appl. Catal., A*, 2009, **371**, 148.
- 48 A. Shaabani, A. Maleki, A. H. Rezayan and A. Sarvary, *Mol. Diversity*, 2011, **15**, 41.
- 49 A. Shaabani, E. Farhangi and A. Rahmati, *Appl. Catal., A*, 2008, **338**, 14.
- 50 A. Shaabani and A. Maleki, *Appl. Catal., A*, 2007, **331**, 149.
- 51 A. Shaabani, A. Rahmati and Z. Badri, *Catal. Commun.*, 2008, **9**, 13.
- 52 W. S. Hummers and R. E. Offeman, *J. Am. Chem. Soc.*, 1958, **80**, 1339.
- 53 W. R. Collins, E. Schmois and T. M. Swager, *Chem. Commun.*, 2011, **47**, 8790.
- 54 E. Buhleier, W. Wehner and F. Vögtle, *Synthesis*, 1978, **2**, 155.
- 55 R. Moors and F. Vögtle, *Chem. Ber.*, 1993, **126**, 2133.
- 56 S. Inagaki, H. Nanbu and L. R. Juneja, *J. Mater. Chem.*, 2006, **16**, 4714.
- 57 M. P. Seah, I. S. Gilmore and S. J. Spencer, *J. Electron Spectrosc. Relat. Phenom.*, 2001, **120**, 93.
- 58 L. Gucci, Z. Schay, G. Stefler and F. Mizukami, *J. Mol. Catal. A: Chem.*, 1991, **141**, 177.
- 59 D. Sun, V. Mazumder, O. Metin and S. Sun, *ACS Nano*, 2011, **5**, 6458.
- 60 T. Mallát, J. Petró, S. Szabó and L. Marczis, *J. Electroanal. Chem. Interfacial Electrochem.*, 1986, **208**, 169.
- 61 R. W. J. Scott, O. M. Wilson, S. K. Oh, E. A. Kenik and R. M. Crooks, *J. Am. Chem. Soc.*, 2004, **126**, 15583.
- 62 A. K. Singh and Q. Xu, *ChemCatChem*, 2013, **5**, 652.
- 63 Y. T. Chu, K. Chanda, P. H. Lin and M. H. Huang, *Langmuir*, 2012, **28**, 11258.
- 64 P. Li, L. Wang and H. Li, *Tetrahedron*, 2005, **61**, 8633.
- 65 R. G. Heidenreich, K. Kohler, J. G. E. Krauter and J. Pietsch, *Synlett*, 2002, 1118.
- 66 H. Sajiki, G. Zhang, Y. Kitamura, T. Maegawa and K. Hirota, *Synlett*, 2005, 619.
- 67 A. Khalafi-Nezhad and F. Panahi, *Green Chem.*, 2011, **13**, 2408.
- 68 L. Rumi, G. M. Scheuermann, R. Mulhaupt and W. Bannwarth, *Helv. Chim. Acta*, 2011, **94**, 966.
- 69 K. R. Reddy, N. S. Kumar, P. S. Reddy, B. Sreedhar and M. L. Kantam, *J. Mol. Catal. A: Chem.*, 2006, **252**, 12.